Study on the Asymmetric Thermodynamic Process of an EV Scroll Compressor

Zibo Zhao[1], Jianhua Wu[1]*, Shuai Zhang[1, 2], Che Wang[1], Jiajing Li[1]

[1]School of Energy and Power Engineering, Xi'an Jiaotong University, Xi'an, Shaanxi, China
(zhaozb0824@stu.xjtu.edu.cn, jhwu@mail.xjtu.edu.cn, wangche0731@outlook.com, xj182000518@stu.xjtu.edu.cn)

[2]Jiangsu Nanfang Changsheng Amperex Technology Co., Ltd, Changzhou, Jiangsu, China
(shuai.zhang@nfcatl.com)

* Corresponding Author

ABSTRACT

The air conditioning system in the TMS of EVs has high energy consumption, which seriously impacts the cruising range of EVs, and this part of the energy consumption mainly comes from the scroll compressor.
The development trend of the EV scroll compressor is towards miniaturization, which results in the compressor often having a shorter scroll wrap and possibly needing to operate at speeds up to nearly 10000 rpm. Furthermore, the smaller built-in volume ratio may cause discharge delay under typical operating conditions. The scroll plate features, including the lengths of the scroll wraps, the shape and position of the ports, and the crescent groove at the beginning of the orbiting scroll, make the fluid flow within the scroll chambers complicated, resulting in the thermodynamic process becoming significantly asymmetric.
To study the asymmetric thermodynamic process of the EV scroll compressor under different operating conditions and speeds, this paper established a corresponding mathematical model of the compressor, which mainly includes the geometry analysis model, the thermodynamic process model considering the bypass flow process, and the valve dynamics model coupled with the former. The thermodynamic process of the scroll compressor was calculated and analyzed. The asymmetric compression characteristics under different working conditions and speeds were revealed.

1. INTRODUCTION

The compressor is the largest energy consumption part in the thermal management system (TMS). After years of technological development and market competition, most compressors currently used in electric vehicles (EVs) are scroll compressors, which have several features as below:

- The length of the scroll wrap is often short enough to reduce the dimension and weight of the scroll plate, which cannot leverage the advantage of multi-chamber compression.
- The bypass structure, some called the intermediate discharge structure, is adopted to reduce the over-compression loss or quickly release the pressures of the scroll chambers when liquid shock occurs. Its structural design and actual effects still need to be reviewed and verified for its weak impact on the over-compression in many prototypes when operating under low-pressure ratio conditions.
- The pressure wave-guide structure (Itoh *et al.*, 1994), named after the crescent groove in this paper, is designed at the beginning of the orbiting scroll in many prototypes, resulting in the compression and discharge processes becoming more complicated due to the additional flow channels.
- To adapt to the various and complex working conditions of the TMS, the compressor operation takes into account a wider pressure ratio and speed range, which also puts forward new requirements for the structural design of compressor components…

The structural features above, including the different lengths of the scroll wraps, the shape and position of the discharge port and bypass ports, and the crescent groove at the beginning of the orbiting scroll, are summarized as the asymmetrical structures of the scroll plate. The asymmetrical structures lead to an asymmetric thermodynamic

process, such as the pressure difference between the scroll chambers on two sides, causing or enhancing the pressure pulsation and leakage loss, and affecting the compressor's performance. Additionally, the stability of the orbiting scroll may also be impacted (Lee, 2003).

However, few papers currently study the impact of asymmetrical structures on the asymmetric thermodynamic process within scroll chambers. Zhao *et al.* (2020) investigated the asymmetric compression phenomenon during the discharge process by the CFD method, and the discharge port was modified to improve this issue. Baumgart *et al.* (2022) optimized the pre-outlet and main-outlet bores by solving a mathematical model, and the asymmetric compression phenomenon was found before the disengagement of the innermost conjugate points.

The entire thermodynamic process still lacks a relatively comprehensive analysis. In this paper, a typical electric vehicle scroll compressor was selected as the research object. A one-dimensional thermodynamic process model of the compressor was established, coupled with the dynamic model of the valves and the force analysis model of the orbiting scroll, the eccentric bushing, and the crankshaft parts. An in-depth analysis was conducted on the asymmetric pressure characteristics of the scroll chambers with the orbiting angle under different pressure ratios and rotational speeds. Besides, the characteristics of the fluid flow in the scroll chambers, the bypass structure, and the crescent groove were studied.

2. MATHEMATICAL MODEL OF THE SCROLL COMPRESSOR

2.1 The geometry analysis method

In this paper, the scroll profile is involute of the circle, with symmetrical arc modification at the beginning. Asymmetrical scroll wraps, where the end angle of the fixed scroll wrap is larger than that of the orbiting scroll wrap, are adopted. The scroll wrap geometry analysis method is based on the generalized profile theory and refers to our previous work (Zhang *et al.*, 2023).

The bypass structure consists of two circular bypass ports and corresponding valves distributed on both sides of the discharge port. For the sake of simplicity, the bypass ports are named bpfi and bpfo according to the adjacent fixed scroll wraps.

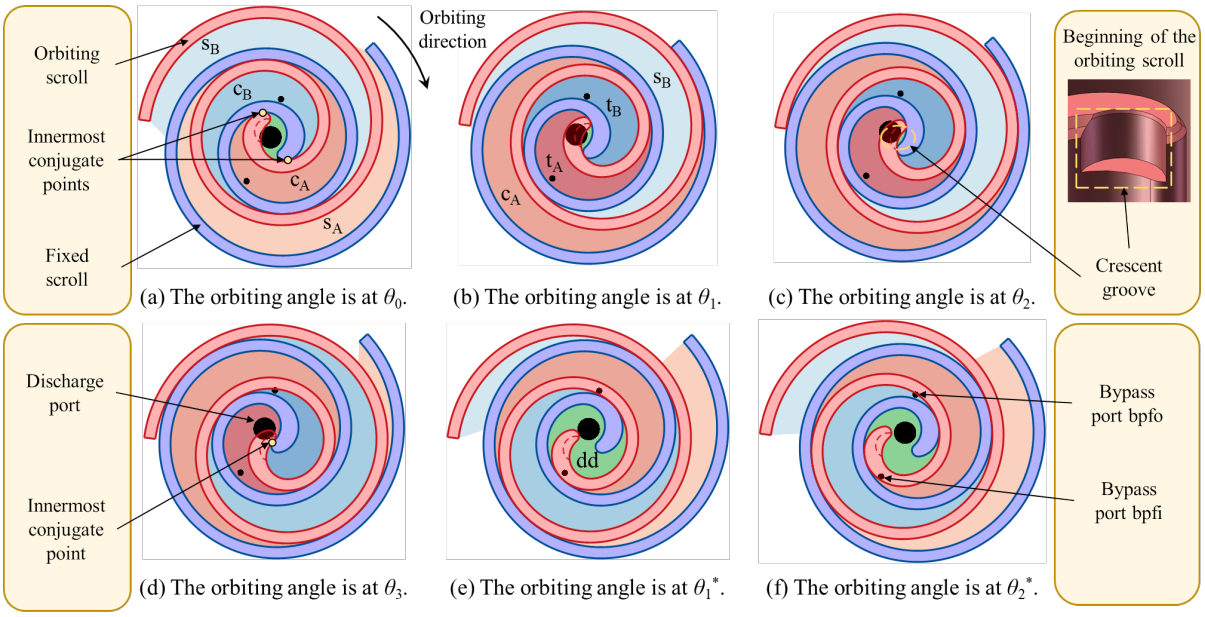

Figure 1: Scheme of the scroll chambers at each special orbiting angle

Similar to the representation method proposed in the past, the scroll chambers formed by the inner side of the fixed scroll and the outer side of the orbiting scroll are represented by the subscript A, and the scroll chambers formed by the inner side of the orbiting scroll and the inner side of the fixed scroll are represented by the subscript B. Several special orbiting angles related to chamber evolution or fluid flow among certain chambers are defined. The schemes of scroll chambers at different special angles are shown in Figure 1.

When the orbiting angle reaches θ_0, the innermost conjugate points coincide with the junction point of the involute and the modified arc. The innermost compression chambers will change from being formed only by the involute to being formed by the involute and the arc after θ_0. Therefore, the innermost compression chambers are named the transition chambers, and the angle θ_0 is called the transition angle.
When the orbiting angle reaches θ_1, the outer side of the orbiting scroll is tangent to the edge of the discharge port, and the chamber t_A will be connected to the discharge port after θ_1.
When the orbiting angle reaches θ_2, the boundary point of the crescent groove coincides with the innermost conjugate point on the inner side of the orbiting scroll. The chamber t_B will be connected to the discharge chamber dd after that.
When the orbiting angle reaches θ_3, the innermost conjugate point pair becomes a point. The innermost conjugate point, on the arc, will disappear awhile, and t_A is connected to t_B directly after θ_3.
For the bypass structure, when the orbiting angle reaches θ_1^*, the inner wrap of the orbiting scroll is tangent to the edge of bpfo, to which the compression chamber c_B will be connected after θ_1^*. It is similar to c_A and bpfi, distinguished by θ_2^*.
As for the special angles, θ_0 and θ_3 can be easily obtained by the geometry characteristics (Zhang *et al*., 2023). The other angles are numerically solved by Boolean operation.

2.2 The mathematical model

To establish the thermodynamics model with a convenient solving method, some assumptions are made as below:

- Neglect the situation of two-phase compression, which means the refrigerant is in the vapor state and the lubricant is in the liquid state.
- The refrigerant and lubricant in the chambers are evenly mixed under the same pressure and temperature, and there is no heat transfer between them.
- Neglect the velocity slip between the refrigerant and the lubricant in chambers.
- Neglect the heat transfer effect between the lubricant and the wall of the scroll wrap.

Based on the assumptions above, three governing equations of the fluid in chambers can be established below:
Conservation of mass

$$\frac{\mathrm{d}m}{\mathrm{d}\theta}=\frac{1}{\omega}\sum_{\mathrm{f}}\left(\dot{m}_{\mathrm{in}}-\dot{m}_{\mathrm{out}}\right) \tag{1}$$

Conservation of species

$$\frac{\mathrm{d}x_{\mathrm{l}}}{\mathrm{d}\theta}=\frac{1}{m}\left[\frac{1}{\omega}\sum_{\mathrm{f}}\left(\dot{m}_{\mathrm{l,in}}-\dot{m}_{\mathrm{l,out}}\right)-x_{\mathrm{l}}\frac{\mathrm{d}m}{\mathrm{d}\theta}\right] \tag{2}$$

Conservation of energy

$$\frac{\mathrm{d}T}{\mathrm{d}\theta}=\frac{\left[\frac{\dot{Q}}{\omega}+\frac{1}{\omega}\sum_{\mathrm{f}}\dot{m}_{\mathrm{in}}\left(h_{\mathrm{in}}-h_{\mathrm{out}}\right)-m\left(h_{\mathrm{g}}\frac{\mathrm{d}x_{\mathrm{g}}}{\mathrm{d}\theta}+h_{\mathrm{l}}\frac{\mathrm{d}x_{\mathrm{l}}}{\mathrm{d}\theta}\right)-T\left(\frac{\partial p}{\partial T}\right)_{\mathrm{v,g}}\left(\frac{\mathrm{d}V}{\mathrm{d}\theta}-v_{\mathrm{g}}\frac{\mathrm{d}m_{\mathrm{g}}}{\mathrm{d}\theta}-v_{\mathrm{l}}\frac{\mathrm{d}m_{\mathrm{l}}}{\mathrm{d}\theta}\right)\right]}{m\left(x_{\mathrm{g}}c_{\mathrm{v,g}}+x_{\mathrm{l}}c_{\mathrm{v,l}}\right)} \tag{3}$$

The dynamic model of the valve is based on the works of Min *et al*. (2018) and Lin *et al*. (2020), and the corresponding equations are established as:

$$\begin{cases}\dfrac{\mathrm{d}y}{\mathrm{d}\theta}=u_{\theta}\\ \dfrac{\mathrm{d}u_{\theta}}{\mathrm{d}\theta}=\dfrac{1}{\omega^2}\left[\dfrac{F_{\mathrm{g}}}{m_{\mathrm{eq}}}-\left(2\zeta\omega_{\mathrm{n}}u_{\theta}+\omega_{\mathrm{n}}^2y\right)\right]\end{cases} \tag{4}$$

The works of Jang *et al*. (2006) and Rak *et al*. (2020) are referred to establish the heat transfer model, which is based on the Dittus-Boelter heat transfer model mainly considering the impact of the orbiting scroll plate motion and the flank leakage. The incompressible flow model (Ishii *et al*., 2006) is adopted to calculate the leakage flow, which is in a simple mathematical form and has been verified by the experiment. The dynamic analysis model is established to consider the effect of the frictional heat (Zhang *et al.*, 2022). The physical parameters of the refrigerant and the lubricant fit into a relationship and are embedded in the program.
The control volumes (CVs) include the scroll chambers, the discharge port (pt), two bypass ports (bp), the chamber behind the valve (bc), and the motor chamber, introducing the heating effects of the motor and the inverter.
The model is solved by the Runge-Kutta-Felhberg method (Bell, 2011).

3. SIMULATION PARAMETERS

The basic parameters of the prototype are listed in Table 1.

Table 1: Basic parameters of the scroll compressor

Parameter	Value	Parameter	Value
Refrigerant type	R134a	Displacement	46 cm^3/r
Base circle radius	2.6 mm	Discharge port diameter	7.0 mm
Orbiting radius	4.7 mm	Bypass port diameter	2.0 mm

Based on the mathematical model above, certain typical cases of the compressor are calculated. The operating conditions of the cases are listed in Table 2.

Table 2: Operating conditions of the scroll compressor

NO.	Suction Pressure [MPa]	Discharge Pressure [MPa]	Rotational Speed [RPM]	Superheating [K]
#1	0.3	0.6	3000	10
#2	0.3	0.6	8000	10
#3	0.3	1.5	3000	10
#4	0.3	1.5	8000	10

4. RESULT AND DISCUSSION

It is specified that the orbiting angle is 0° when the suction chamber s_A is closed. The pressure characteristics of the chambers and ports are analyzed.

4.1 Result of operating condition #1 (low-pressure ratio & low rotational speed)

It illustrates the pressure changes at the low-pressure ratio and low rotational speed condition in Figure 2. It can be discovered that the pressure difference results from the different wrap lengths of the orbiting and fixed scrolls between chambers A and B. Whatever, the difference is almost constant before θ_1.
The pressure growth rate of chamber A decreases after θ_1, making the pressure difference gradually smaller, and then chamber B's pressure becomes greater than chamber A's. It is the connection between pt and t_A that causes this phenomenon. The fluid in t_A, of which the pressure is greater than that of pt, flows towards pt, increasing the pressure of pt. The pressure of t_A, however, increases first and then decreases rather than decreases directly. This is caused by the connected area being small to begin with.
When the orbiting angle reaches θ_2, t_B is connected to dd through the crescent groove, and the fluid in t_B begins to flow towards dd driven by the pressure difference. In the final stage of the discharge process, the pressure of dd rises again, and the pressure growth of t_B becomes slower.
The chambers t_B and dd are no longer connected to pt around θ_3, so the pressure of the two chambers increases rapidly at a rate close to the early stage of compression. After θ_3, the connected area between t_A and t_B rises quickly,

and the fluid is mixed by the pressure difference in the two chambers. Finally, the physical properties are identical, and the connected two chambers form a new discharge chamber.
The discussion of the bypass structure is then performed. The bypass port bpfo is connected to the chamber c_B after θ_1^*, and the pressure of bpfo quickly drops to be consistent with c_B. A similar situation occurs at θ_2^* for bpfi. There is a large overlapping area between the pressure curves of the bypass ports and the corresponding compression chambers, and in this area, the ports and the chambers are in a connected state.
Under this operating condition, since the pressure of pt is always higher than that of bc, the discharge valve is always open. However, the bypass process is shorter.
It can be seen from the pressure of the scroll chambers and the bypass ports that the bypass structure does not function very effectively. The main reason for this is that the diameter of the bypass ports is too small to allow the over-compressed fluid to be fully discharged.

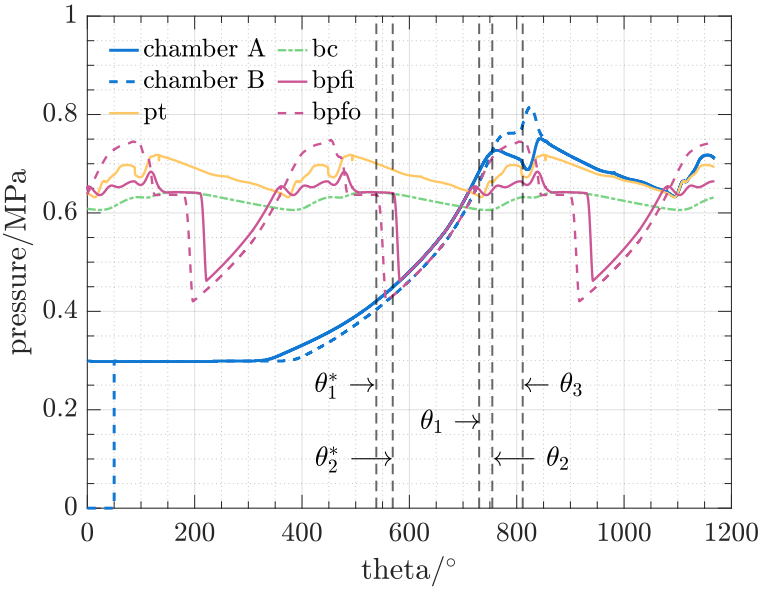

Figure 2: Pressure in different CVs at operating condition #1

4.2 Result of operating condition #2 (low-pressure ratio & high rotational speed)

The pressure changes at the low-pressure ratio and high rotational speed condition are shown in Figure 3. At high rotational speed, the over-compression phenomenon of the compressor is severe. The pressure peaks in dd and pt are almost twice the nominal discharge pressure, and the discharge valve is always open.
The pressure of the chamber t_A is not significantly affected by the pressure of pt after θ_1. On the one hand, because pt and dd have small volumes, their impact on t_A is limited. On the other hand, at the end of the discharge process in the previous cycle, the pressure of pt dropped rapidly; the angle change from θ_1 to the angle at which the pressure balance achieved between t_A and pt is small. When their pressure is balanced, the connected area between t_A and pt only accounts for 23% of the total area of pt; the pressure loss is significant at high rotational speed, and the actual mass exchange between them is limited.
The reasons above can similarly explain why the pressure of chamber B is not significantly affected after θ_2, though chamber B and dd have been connected.
The connected area between t_A and pt is large enough around θ_3, and the pressure of t_A rises slowly; t_B is no longer connected to pt, and its pressure increases at the same rate as at the beginning of the compression process.
Due to the significant pressure loss, the function of the bypass structure is further limited. The bypass process is much shorter than that at condition #1.

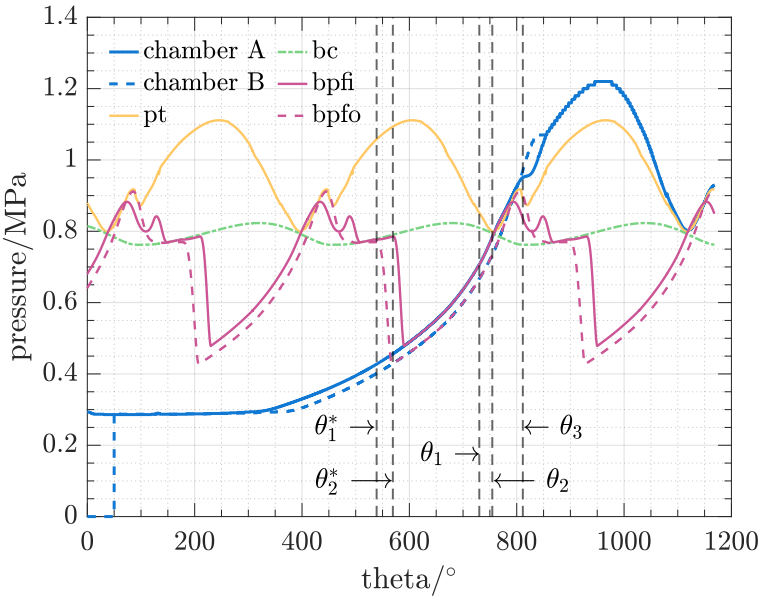

Figure 3: Pressure in different CVs at operating condition #2

4.3 Result of operating condition #3 (high-pressure ratio & low rotational speed)

As shown in Figure 4, compared with the low-pressure ratio operating condition #1, the phenomenon of asymmetric compression of the two chambers still exists in the medium or high-pressure ratio condition.

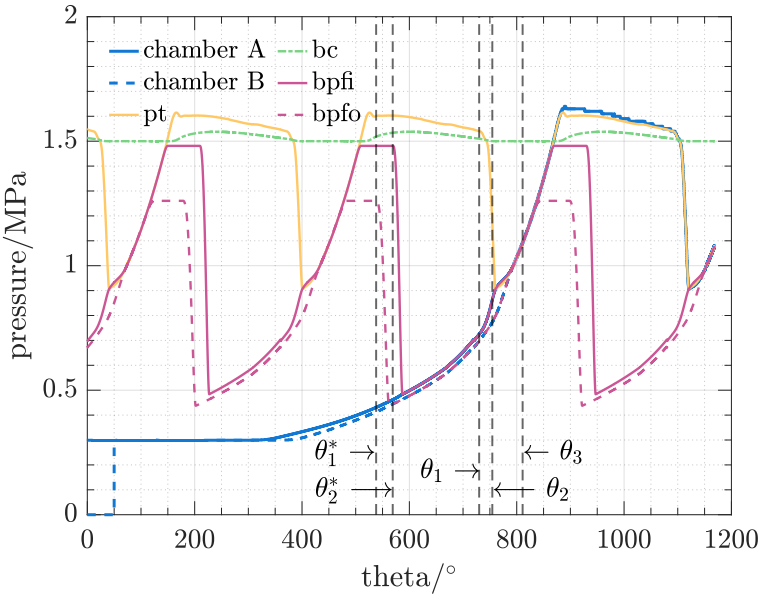

Figure 4: Pressure in different CVs at operating condition #3

In the early stage of the compression process, asymmetric compression is caused by the asymmetric scroll wraps, which is consistent with the cause of the phenomenon under condition #1; in the middle and final stages of the compression process, the pressure of chamber A is always higher than that of chamber B, which is different from the situation under the low-pressure ratio condition. Different phenomena reflect the different asymmetric compression mechanisms under different pressure ratio conditions.

After θ_1, since the pressure of pt is much higher than c_A's, the fluid in pt quickly flows to c_A, causing the pressure of pt to drop rapidly and the pressure of chamber A to increase faster. Until the pressures of pt and c_A are balanced, the

pressure growth rate in chamber A returns to the state before θ_1. The discharge valve closes, and the exhaust process is complete for the pressure difference.
When the orbiting angle reaches θ_2, the pressure drop is formed from c_A, pt, dd to c_B, driving the flow of the fluid. Due to the small connected area of the crescent groove, the pressure difference between dd and c_B is significant in a short time. The connected area between pt and c_A is not large, and there is still a slight pressure difference between them. The pressures of dd and pt are almost the same.
As the fluid flows, the pressures of the four CVs reach equilibrium, and the orbiting angle at which the equilibrium is reached is ahead of θ_3.
When the pressure of pt exceeds the pressure of bc, the discharge valve gradually opens, and the compressor begins to exhaust. In the initial stage of the discharge process, the area of the valve gap is small, causing the pressures of dd and pt to increase further, resulting in the over-compression phenomenon.

4.4 Result of operating condition #4 (high-pressure ratio & high rotational speed)

As shown in Figure 5, compared with the low rotational speed condition #3, the pressure under high speed has two main characteristics:

- The pressures of chambers A and B have not yet reached equilibrium at θ_3.
- The over-compression phenomenon of the compressor is prominent during the discharge process.

The above phenomena are all caused by excessive pressure loss of the fluid flow at high speeds.
As the pressure ratio increases, regardless of the speed, the bypass structure does not affect the pressure of the chambers. The reason for this phenomenon is that under medium and high-pressure ratio conditions, when the bypass ports and the scroll chamber are connected, the pressures of the scroll chambers are consistently low, and the pressure of the bypass ports does not exceed the pressure of bc, so the bypass valves cannot be opened.
As the rotational speed increases, the over-compression loss of the compressor becomes larger and larger. However, since the bypass structure cannot function under medium or high-pressure ratios and high rotational speeds, the bypass structure is also helpless in reducing the over-compression loss.

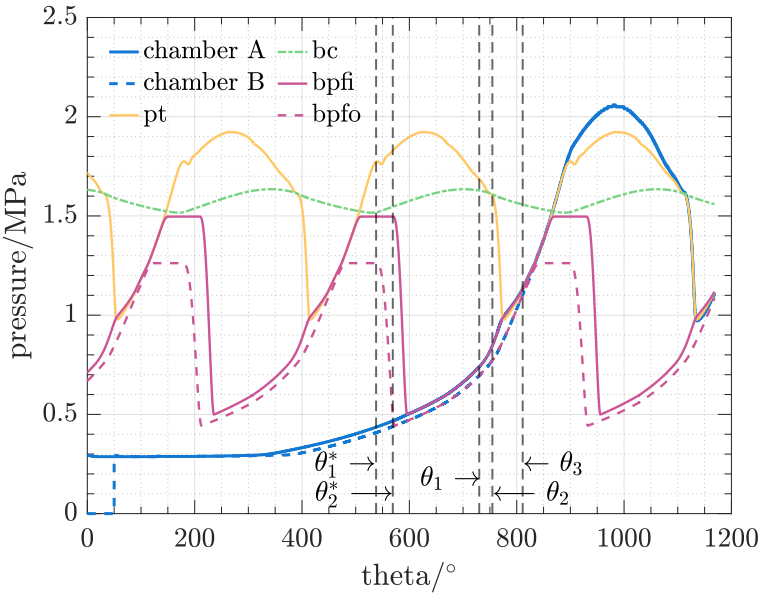

Figure 5: Pressure in different CVs at operating condition #4

The above comparison shows that the bypass structure can only function under low-pressure ratio conditions. More specifically, the built-in volume ratio of the bypass structure is defined.

$$Vr_{bp} = \frac{V_s}{V_{c,bp}} \tag{5}$$

From Equation (5), it can be quantitatively determined that under what pressure ratio the bypass structure could function in theory.

5. CONCLUSIONS

This paper calculates and analyzes the thermodynamic process within the electric vehicle scroll compressor. Six aspects of the research are summarized below:

- The asymmetric profile slightly impacts the pressure difference of the chambers on both sides due to the different lengths of the scroll wraps.
- The discharge port and crescent groove are the main reasons for the significant pressure difference between the chambers on both sides.
- Under different pressure ratios, the characteristics of the pressure difference between the chambers on both sides are different, mainly determined by the built-in volume ratio of the compressor.
- Similarly, the bypass structure is limited by the built-in volume ratio of the bypass structure and only functions under low-pressure ratios. Due to the small bypass port diameter, the pressure release is limited.
- The pressure difference between the chambers on both sides is less affected by the rotational speed.
- At high rotational speed, the over-compression loss is significant. When the application focuses on high-speed working conditions, the discharge port should be modified to reduce the pressure loss.

NOMENCLATURE

p	pressure	(Pa)
T	temperature	(K)
u	velocity	(m/s)
V	volume	(m^3)
Vr	volume ratio	(–)
v	specific volume	(m^3/kg)
x	mass fraction	(–)
y	displacement of the valve	(m)
θ	orbiting angle	(rad)

Subscript

bc	chamber behind the valve
bp	bypass port
c_A/c_B	compression chambers
dd	discharge chamber
g	refrigerant
in	inlet
l	lubricant
out	outlet
pt	discharge port
s_A/s_B	suction chambers
t_A/t_B	transition chambers

REFERENCES

Itoh, T., Fujitani, M., & Takeda, K. (1994). Investigation of Discharge Flow Pulsation in Scroll Crompressors. International Compressor Engineering Conference, 1056.

Ishii, N., Bird, K., Sano, K., Oono, M., Iwamura, S., & Otokura, T. (1996). Refrigerant Leakage Flow Evaluation for Scroll Compressors. International Compressor Engineering Conference, 1175.

Lee, B., 2003, スクロール圧縮機における非対称ラップの挙動および漏れ特性に関する研究, Diss. Shizuoka University, Shizuoka, Shizuoka-ken, Japan, 98 p.

Jang, K., & Jeong, S. (2006). Experimental investigation on convective heat transfer mechanism in a scroll compressor. International Journal of Refrigeration, 29(5), 744–753.

Bell, I., (2011). Theoretical and Experimental Analysis of Liquid Flooded Compression in Scroll Compressors, Diss. Purdue University, West Lafayette, Indiana, USA, 622 p.
Min, B., Na, S., Yang, J., & Choi, G. (2018). Geometric correlation of discharge coefficients for discharge valve system in rolling piston rotary compressor. Journal of Mechanical Science and Technology, 32(8), 3943–3954.
Lin, J., Lian, Y., & Wu, J. (2020). Numerical investigation on vapor-liquid two-phase compression in the cylinder of rotary compressors. Applied Thermal Engineering, 170, 115022.
Rak, J., & Pietrowicz, S. (2020). Internal flow field and heat transfer investigation inside the working chamber of a scroll compressor. Energy, 202, 117700.
Zhao, R., Li, W., & Zhuge, W. (2020). Unsteady characteristic and flow mechanism of a scroll compressor with novel discharge port for electric vehicle air conditioning. International Journal of Refrigeration, 118, 403–414.
Baumgart, R., & Aurich, J. (2022). Optimization of the Pre-Outlet and Main-Outlet Bores in Scroll Compressors. International Compressor Engineering Conference, 1388.
Zhang, S., Wu, J., Wang, C., & Li, J. (2022). A dynamic model for pin coupling anti-rotation mechanism of automotive scroll compressor. Proceedings of the Institution of Mechanical Engineers, Part E: Journal of Process Mechanical Engineering, 095440892211162.
Zhang, S., Wu, J., Wang, C., Zhong, H., & Zhao, Z. (2023). Study on a variable wall thickness profile of electric scroll compressor used for automobile air conditioner. Proceedings of the Institution of Mechanical Engineers, Part A: Journal of Power and Energy, 237(2), 294–307.